

Interstellar Extinction in the Milky Way Galaxy

Edward L. Fitzpatrick

Villanova University, 800 Lancaster Avenue, Villanova, PA 19085

ABSTRACT

I review the basic properties of interstellar extinction in the Milky Way galaxy, focusing primarily on the wavelength dependence within the IR through UV spectral region. My primary goal is to review the evidence supporting the idea that Galactic extinction curves can be considered a 1-parameter family characterized by their value of $R_V \equiv A_V/E(B - V)$. Based on analysis of new (i.e., *2MASS*) and old (i.e., *IUE*) data for ~ 100 sightlines, I show that the UV, optical, and IR wavelength regimes do display coherent variations, but with too much intrinsic scatter to be considered truly correlated. A 1-parameter family can be constructed which illustrates these broad trends, but very few individual sightlines are actually well-reproduced by such a family and disagreement with the mean trends is not a sufficient condition for “peculiarity.” Only a very small number of extinction sightlines stand out as truly peculiar. It is likely that simple variations in the mean grain size from sightline to sightline are responsible for much of the coherent variability seen in Galactic extinction, and might also explain the “peculiar” extinction long-noted in the Magellanic Clouds.

1. Introduction

This conference is a testament to the wide ranging impact of dust grains on the properties of the interstellar medium and to the rich variety of research opportunities in the interstellar dust field. Among these studies, interstellar extinction — the absorption and scattering of light by grains — often plays a central role. The ability of grains to transmit, redirect, and transmute electromagnetic energy is enormously important to the physics of interstellar space. The wavelength dependence of extinction provides important diagnostic information about the physical properties of grain populations, and often serves as a first test for possible grain models. And, perhaps most far-reaching, interstellar extinction profoundly limits our ability to study the universe. It is certainly fair to say that many more astronomers care about extinction, than care about the dust grains that produce it!

In recent history there have been a number of excellent review articles about, or including, the basic properties of interstellar extinction in the Milky Way galaxy (e.g., Savage & Mathis 1979;

Massa & Savage 1989; Draine 1995; and Draine 2003). In addition, the book by Whittet (2003) provides a valuable general reference. Since the pace of research in the extinction field is such that the astronomical community is not really demanding a new review article every year, I have taken a liberal approach to the notion of a “review.” In this paper, my aim is principally to review an idea, rather than a field. The idea is that — despite the wide range of spatial variations present — the λ -dependence of Galactic extinction can be viewed as a smoothly varying 1-parameter family and that the normalcy of an extinction sightline can be judged by how well it fits into this family. In a sense, this article is a natural follow-up to that by Massa & Savage (1989) presented at the Santa Clara dust meeting. Massa & Savage gave a comprehensive review of the detailed λ -dependence of extinction and included a discussion of the then-recent results of Cardelli, Clayton, & Mathis (1988, 1989) who first showed a relationship between extinction properties in the IR/optical and in the UV. It is these results which have given rise to the 1-parameter family scenario.

I begin this article with a brief description of the basic properties and terminology of Galactic extinction (§2) and then give a short history of the key developments which provide the primary background for this paper (§3). In §4, I will examine the evidence for a multi-wavelength connection between IR, optical, and UV extinction, i.e., the issue of a 1-parameter family, based on a new analysis of UV, optical, and IR data. The analysis incorporates a threefold increase over past studies in the number of sightlines for which IR and UV data are combined, and utilizes a new technique for deriving extinction curves which promises to allow precise extinction studies to be extended to more lightly-reddened sightlines than previously possible. Finally, in §5 I will revert to classical “review-mode” and note a number of recent programs and results which are helping to clarify our view of the λ -dependence of Galactic extinction and the relationship between extinction properties and interstellar environment.

2. The Extinction Basics

While the ultimate interpretation of results from extinction studies may be very complex, the measurements themselves for Galactic (and many extra-Galactic) sightlines are, in principle, straightforward. The most commonly used technique for deriving the λ -dependence of extinction, the “pair method,” is illustrated in idealized form in Figure 1. Measuring the extinction produced by an interstellar cloud requires photometric or spectrophotometric observations of the spectral energy distribution (SED) of some astronomical object — usually a star — located behind the cloud and identical measurements of an identical object located at an identical distance, but unaffected by interstellar dust. The total extinction in magnitudes at each wavelength A_λ (which is essentially a measure of the optical depth τ_λ) is then simply computed from the ratios of the SEDs as shown in Figure 1. Note that the assumption implicit in this discussion is that the star is located far from the interstellar cloud (as indicated in Figure 1) and that no photons are scattered *into* the line of sight. Such an assumption is not necessarily valid in the case of extinction produced by circumstellar material.

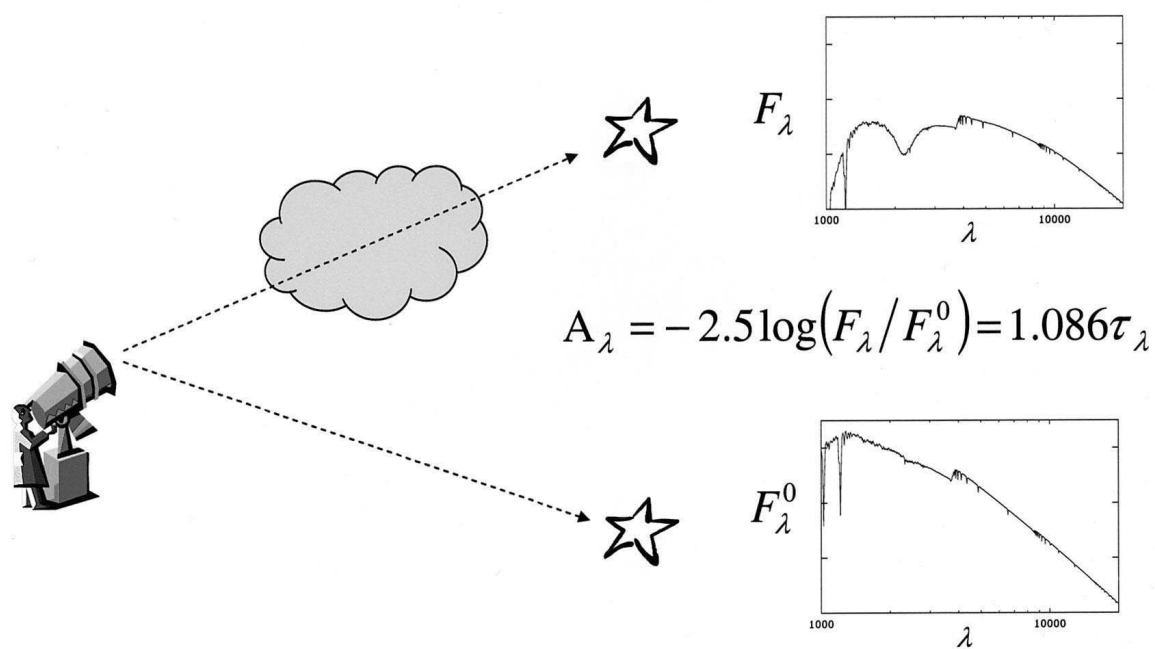


Fig. 1.— A schematic illustration of the “Pair Method,” the principal technique used to study Milky Way extinction.

Because reddened/unreddened star pairs are nearly never at the same distance and, in fact, the stellar distances are usually poorly determined, the total extinction A_λ is rarely computed directly. Instead, the stellar SEDs are usually normalized by the flux in a common wavelength region before computing the extinction. The usual choice for this is the optical V band. This normalized extinction $A_{\lambda-V}$ (computed by substituting F_λ/F_V and F_λ^0/F_V^0 into the equation in Figure 1) is also known as the color excess $E(\lambda - V)$ and is related to the total extinction by $E(\lambda - V) = A_\lambda - A_V$.

To effectively compare the λ -dependence of extinction among sightlines with very different quantities of interstellar dust, the color excess $E(\lambda - V)$ itself must be normalized by some factor related to the amount of dust sampled. The optical color excess $E(B - V)$ is usually employed for this purpose. This second normalization yields the most commonly found form for observed “extinction curves”, namely $E(\lambda - V)/E(B - V)$. This normalized extinction is related to the total extinction A_λ through the relation $E(\lambda - V)/E(B - V) = A_\lambda/E(B - V) - A_V/E(B - V)$. The quantity $A_V/E(B - V)$, i.e., the ratio of total extinction to color excess in the optical region, is usually denoted R_V . If its value can be determined for a line of sight, then the easily-measured normalized extinction can be converted into total extinction.

It has been noted often that $E(B - V)$ is a less-than-ideal normalization factor. Certainly a physically unambiguous quantity, such as the dust mass column density, would be preferred, or even a measure of the total extinction at some particular wavelength, such as A_V . However, the issue is simply measurability. We have no model-independent ways to assess dust mass and total extinction requires either that we have precise stellar distances or can measure the stellar SEDs in the far-IR where extinction is negligible. While IR photometry is now available for many stars through the *2MASS* survey, the determination of total extinction from these data still requires assumptions about the λ -dependence of extinction longward of $2\mu\text{m}$ and can be compromised by emission or scattering by dust grains near the stars. In this paper, all the observed extinction curves will be presented in the standard form of $E(\lambda - V)/E(B - V)$. Only in the case of model curves, and for illustrative purposes, will alternate normalizations be employed.

The quality of a pair method extinction curve clearly depends on how well a reddened object can be matched with an unreddened comparison object. Massa et al. (1983) discuss the effects and magnitude of “mismatch errors” on extinction curves. In general, mismatch effects become less important as the amount of extinction increases, and strongly limit our ability to probe the λ -dependence of extinction in lightly reddened sightlines, such as through the nearby interstellar medium and the galactic halo. In §4, I will present results based on the substitution of stellar atmosphere models for the unreddened member of a pair method star team. Along with a number of other advantages, this technique promises to greatly improve the accuracy of extinction curves derived for low-reddening sightlines.

Several decades of work utilizing pair method extinction curves spanning the near-IR through UV spectral domain have provided a good estimate of the “average” λ -dependence of extinction in

the Milky Way galaxy. (I will defer describing what I mean by “average” until §3 below). Figure 2 shows the familiar shape of this “Average Galactic Extinction Curve”, plotted as $E(\lambda - V)/E(B - V)$ vs. inverse wavelength. This type of presentation was clearly invented by UV astronomers to emphasize that spectral region, but also has the advantage of being essentially a plot of normalized extinction cross section vs. photon energy. The Average Curve itself is shown by the thick solid and dashed curve, with a number of specific features labeled. I use the solid curve to denote the spectral regions where I think the form of the extinction is particularly well-determined. These are the IR 1.25–2.2 μm region (based on *2MASS JHK* photometry), the optical 5500–3600 \AA region (based on *UBV* and *uvby* photometry) and the UV 2700–1150 \AA region (based on *IUE* satellite spectrophotometry).

The most prominent feature in the curve is the “bump” at 2175 \AA . This has been shown to be a pure absorption feature with a Lorentzian-like cross section, and likely arises from a specific physical process occurring on a specific — although currently unidentified — type of dust grain (see §3). The mean profile of the bump is shown by the dash-dot curve at the bottom of the figure. If the profile of the bump is removed from the extinction curve, the underlying extinction in its vicinity is seen to be linear and its slope can be used to characterize the steepness of UV extinction (“UV slope” in Figure 2). At wavelengths shortward of ~ 1500 \AA the extinction departs from the linear extrapolation, rising more rapidly and generally with pronounced curvature (“FUV rise” in Figure 2).

Probably the most outstanding observational characteristic of interstellar extinction is its spatial variability. I show this graphically in Figure 3 where analytic fits to 96 Galactic extinction curves are overplotted, in the form $E(\lambda - V)/E(B - V)$. Only the highly constrained IR, optical, and UV spectral regions are shown. These curves were produced as part of the analysis discussed in §4 below, and their details will be discussed there. Here they simply serve to demonstrate the degree of variability found along Milky Way sightlines. This variability is a two-edged sword. It can provide endless misery to those who seek to correct astronomical observations for the effects of extinction, but also a wealth of data for those who model the interstellar dust grain populations. The extinction variations presumably reflect general differences in the grain populations from sightline to sightline. Understanding how the various spectral regions of the curves relate to each other and how they respond to changes in the interstellar environments can provide information critical for characterizing interstellar grains.

3. A Brief History

A detailed history of the development of our understanding of interstellar extinction is beyond the limited scope I have set for this article. In this section I will outline only a few key items which play a role in the re-analysis of Galactic extinction data to be presented in §4.

The λ -dependence of IR and optical extinction has been studied extensively using ground-

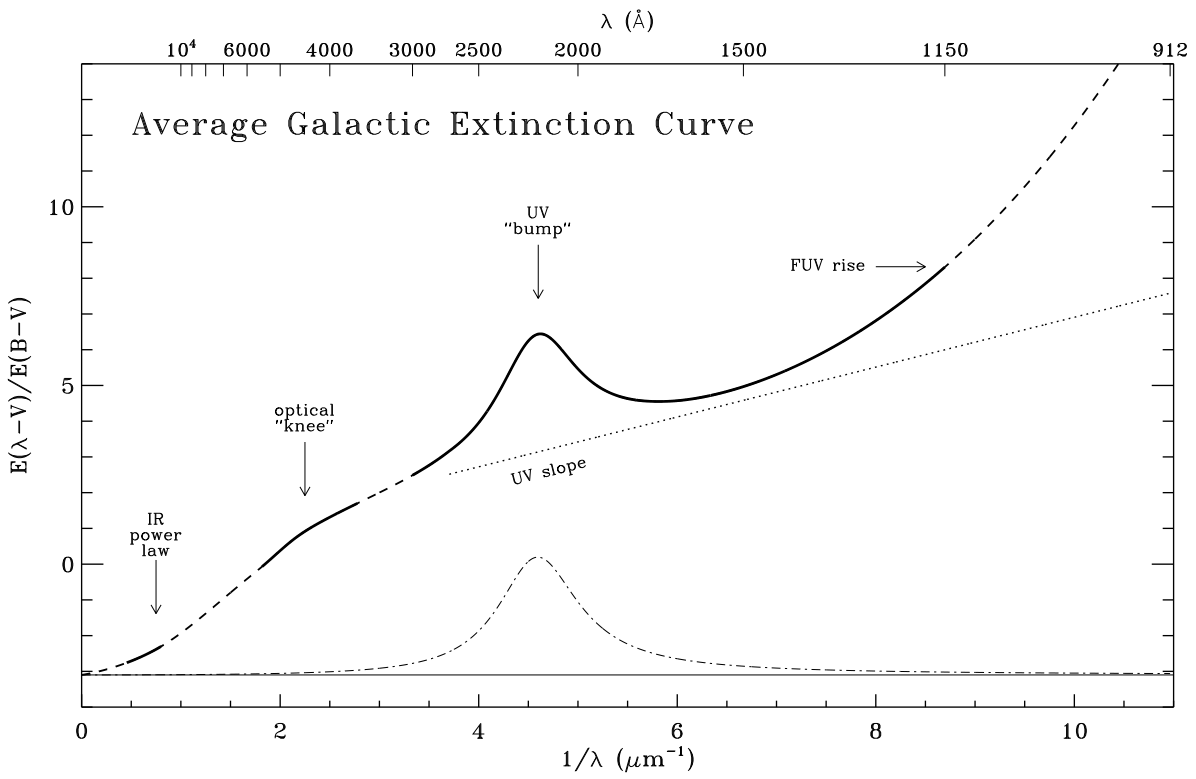


Fig. 2.— The average Milky Way extinction curve, corresponding to the case $R_V = 3.1$, as computed by Fitzpatrick 1999. See the discussion in §2.

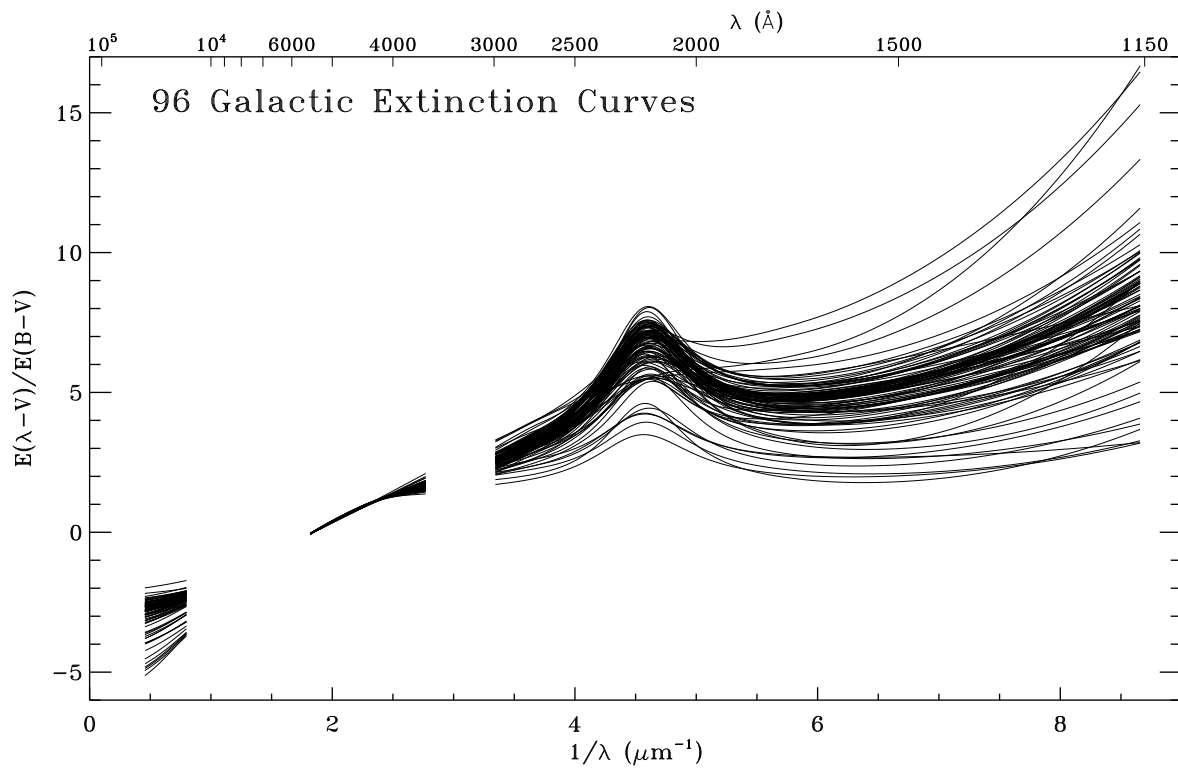


Fig. 3.— Analytical representations of the 96 IR-through-UV extinction curves to be discussed in §4. These illustrate the wide range of extinction properties observed in the Milky Way.

based photometry and sightline-to-sightline variations have long been recognized (e.g., Johnson 1965). These variations can be characterized by their R_V values, which range from ~ 2 to ~ 5.5 for sightlines through the diffuse ISM, with a mean value of ~ 3.1 . The shape of the extinction curve at wavelengths longward of $\sim 1.2 \mu\text{m}$ (i.e., the J band) has been suggested as invariant and universal, following a power law dependence proportional to $\lambda^{-1.84}$ (see the discussion in Whittet 1992).

UV extinction measurements require space-based observations and date back to the late 1960's. The 2175 Å bump was discovered by Stecher (1969) and early observations clearly revealed the presence of sightline-to-sightline variations in the λ -dependence of UV extinction. Soon after, measurements of the UV component of the diffuse galactic light revealed a broad minimum in the scattering albedo centered near 2200 Å, indicating the bump to be an absorption feature (Witt & Lillie 1973). The large spectrophotometric database accumulated by the *IUE* satellite over its long operational lifetime (1978-1996) has provided the best resource for studying UV extinction (see references in Fitzpatrick 1999) and these data are the source of the UV curves shown in Figure 3.

Despite the daunting degree of variation present in Figure 3, the extinction curves do follow some rules and do not assume arbitrary appearance. Savage (1975) first demonstrated that the shape of the 2175 Å bump is well represented by a Lorentzian function. Fitzpatrick and Massa (1986) later showed that, although the strength and width of the bump vary markedly in the ISM, it always retains its Lorentzian-like form and has a nearly invariant central peak position. Fitzpatrick and Massa (1986, 1988, and 1990) also showed that the whole range of known UV extinction curves could be reproduced extremely well by a single analytical expression with a small number of free parameters. This expression consists of (1) a Lorentzian-like bump term (requiring three parameters, corresponding to bump FWHM γ , position x_0 , and strength c_3), (2) a linear term underlying the bump and extrapolated into the far-UV (two parameters, the intercept c_1 and slope c_2), and (3) a far-UV curvature term (one parameter, a scale factor c_4). As far as I know, it is still true that *all* UV extinction curves measured so far can be reproduced with this parameterization scheme to a level consistent with observational error.

Cardelli, Clayton, & Mathis (1988, 1989; and see also Mathis & Cardelli 1992) were the first to demonstrate a link between UV extinction and that in the optical/IR region by showing that R_V correlates with the level of UV extinction. Essentially, sightlines with large R_V values tend to have low UV extinction, and vice versa. These results were important in demonstrating a degree of coherent behavior over the full wavelength range observed for interstellar extinction and for providing a simple recipe for determining a meaningful average extinction curve. I.e., since it is well-established that the mean value of R_V in the diffuse ISM is ~ 3.1 , it is reasonable to define the Average Galactic Extinction Curve as that which corresponds to $R = 3.1$. This is how the curve in Figure 2 was defined.

A comparison of the Cardelli et al. R_V values with the UV extinction curve parameters of Fitzpatrick & Massa suggests that — while other effects are present — the primary basis of the correlation discovered by Cardelli et al. is a relationship between $1/R_V$ and the UV slope

component (see also Jenniskens & Greenberg 1993). Thus the general R_V -dependence of extinction can be distilled to the simple statement that when extinction curves are intrinsically steep in the optical (i.e., large $1/R_V$) they remain steep in the UV (large UV slope), and vice versa. Based on this, Fitzpatrick (1999) produced a much simplified formulation of the R_V -dependence which reproduced the main effects seen by Cardelli et al.

4. A New Look At Old Data or “Is Galactic Extinction Really a 1-Parameter Family?”

Since the early 1990s, there has been very little new data to advance our basic understanding of the multi-wavelength behavior of Galactic interstellar extinction. The *IUE* database was complete by then, optical photometry had already been available for all stars with UV extinction curves, and Cardelli et al. had already exploited virtually all the IR data available for stars with UV extinction curves. This latter point is significant since the Cardelli et al. results are based on data for only 29 stars, out of the several hundred for which UV extinction curves might be derived. What *has* changed over the last 10 years, in my view, is the *perception* of the R_V -dependence discovered for Galactic extinction curves. Increasingly, Galactic extinction curves are referred to as a “1-parameter family” (with R_V as the parameter) and the degree to which a given curve agrees with Cardelli et al.’s (or Fitzpatrick’s 1999) enunciation of the R_V -dependence used as a test of its normalcy.

The time is now right to reexamine the whole issue of the connection between IR, optical and UV extinction. The primary driver for this is the recent All-Sky Data Release from the *2MASS JHK* photometric survey, which allows the determination of R_V for nearly all the stars in the UV extinction database. A secondary motivation for me is the recent development by Derck Massa and myself of a technique for utilizing stellar atmosphere models to derive extinction curves for reddened stars, rather than relying on unreddened standard stars. The technique is described by Fitzpatrick & Massa (1999) and had been utilized in a number of studies of eclipsing binary stars in the Large Magellanic Cloud (see Fitzpatrick et al. 2003 and references within). The benefits to this technique are numerous, including: 1) the elimination of the subjective process of determining the pair method standard; 2) a large reduction in mismatch error in the resultant extinction curves; 3) the ability to determine reliable extinction curves for lower E(B-V) sightlines than possible previously; and 4) the ability to determine reliable UV extinction curves for later type stars (i.e., as cool as early-A) than previously possible. The principal drawback is that the stars to which the technique can be applied must be restricted to the spectral domain in which the models have been shown to precisely and accurately reproduce the stellar SEDs. Currently this forces us to consider only main sequence stars in the late-O through early-A range.

4.1. The Data

Massa and I are currently producing near-IR through UV extinction curves for the several hundred stars in the *IUE* database which are amenable to our technique and a full description of the results is being prepared. In this article, I present the first results from a core sample of 96 stars. These consist of the stars in the atlas of Fitzpatrick & Massa (1990), plus the study by Clayton & Fitzpatrick (1987) of the Trumpler 37 region, plus a number of other sightlines not part of either of those studies, including HD27778, HD29647, HD294264, Brun 885, HD38023, HD38051, HD62542, HD210072, and HD210121. Several O stars from the Fitzpatrick & Massa (1990) sample were eliminated from consideration (HD48099, HD167771, HD199579, HD229296, Trumpler 14 #20, and CPD–59 2600) because their strongly developed C IV stellar wind lines suggested that the hydrostatic stellar atmosphere models being utilized were likely inappropriate.

The analysis technique is described in detail in the references listed above. In brief, it consists of modeling the observed stellar SEDs by combining model atmosphere fluxes with a flexible description of the shape of the IR-through-UV extinction curve. The output of the fit includes the stellar properties (potentially T_{eff} , $\log g$, $[m/H]$, and $v_{microturb}$) and the set of parameters which describe the shape of the extinction curve. In the IR, at wavelengths longward of $1 \mu\text{m}$, we assume the extinction to follow a power law form given by $A_\lambda/E(B-V) = K \times \lambda^{-\alpha}$, where both the scale factor K and the exponent α may be determined by the fit. In the UV, at wavelengths shortward of 2700 \AA , we adopt the 6-parameter fitting function from Fitzpatrick & Massa (1990) described in §3 above. All 6 parameters are determined by the fit. The UV and IR regions are linked by a cubic spline interpolation passing through optical anchor points located near the V , B , and U effective wavelengths. The values of these 3 spline points are strongly constrained by the optical photometry, the value of R_V , and the normalization imposed on the curves, and are all determined by the fit, along with R_V itself. The 6-parameter UV fitting function is restricted to $\lambda < 2700 \text{ \AA}$ because the assumption of a linear component underlying the bump begins to breakdown towards longer wavelengths. This effect can be seen (although it was not recognized at the time) in Figure 2 of Fitzpatrick & Massa (1988).

Our primary datasets are *IUE* spectrophotometry in the UV, *2MASS* photometry in the IR, and *UBV* and *uvby β* photometry in the optical. We use Kurucz’s ATLAS9 atmosphere models to represent the surface fluxes of the B stars and the Lanz & Hubeny (2003) non-LTE models for the O stars.

Figure 4 shows examples of best-fitting SED models for five of the stars in the current sample. The fitting procedure is clearly capable of reproducing the observed SEDs at a level consistent with observational error. Figure 5 shows the extinction curves derived from the SED fits for 11 of the stars, including those in Figure 4. (The parameterized versions of whole set of 96 extinction curves were already shown in Figure 3.) The full set of SED fitting results and extinction curves will be published by Fitzpatrick & Massa (in preparation).

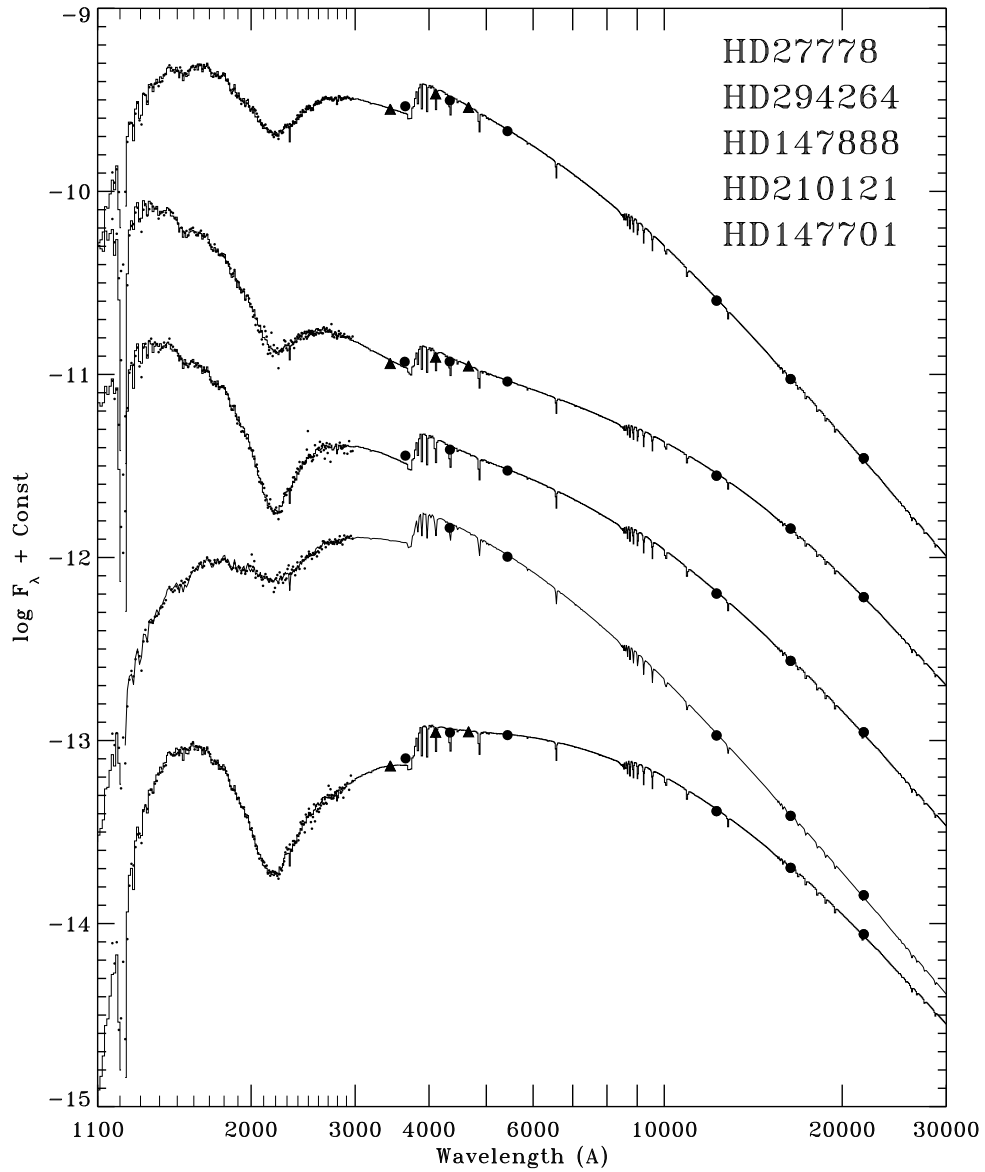


Fig. 4.— Five examples of the fits to reddened star SEDs. IR data are *2MASS* photometry, optical data are *UBV* (circles) and *uvb* (triangles) photometry, and UV data are *IUE* spectrophotometry. The solid curves are the best-fitting stellar atmosphere models reddened by extinction curves whose form is determined by the fitting procedure. The SEDs have been shifted vertically for clarity.

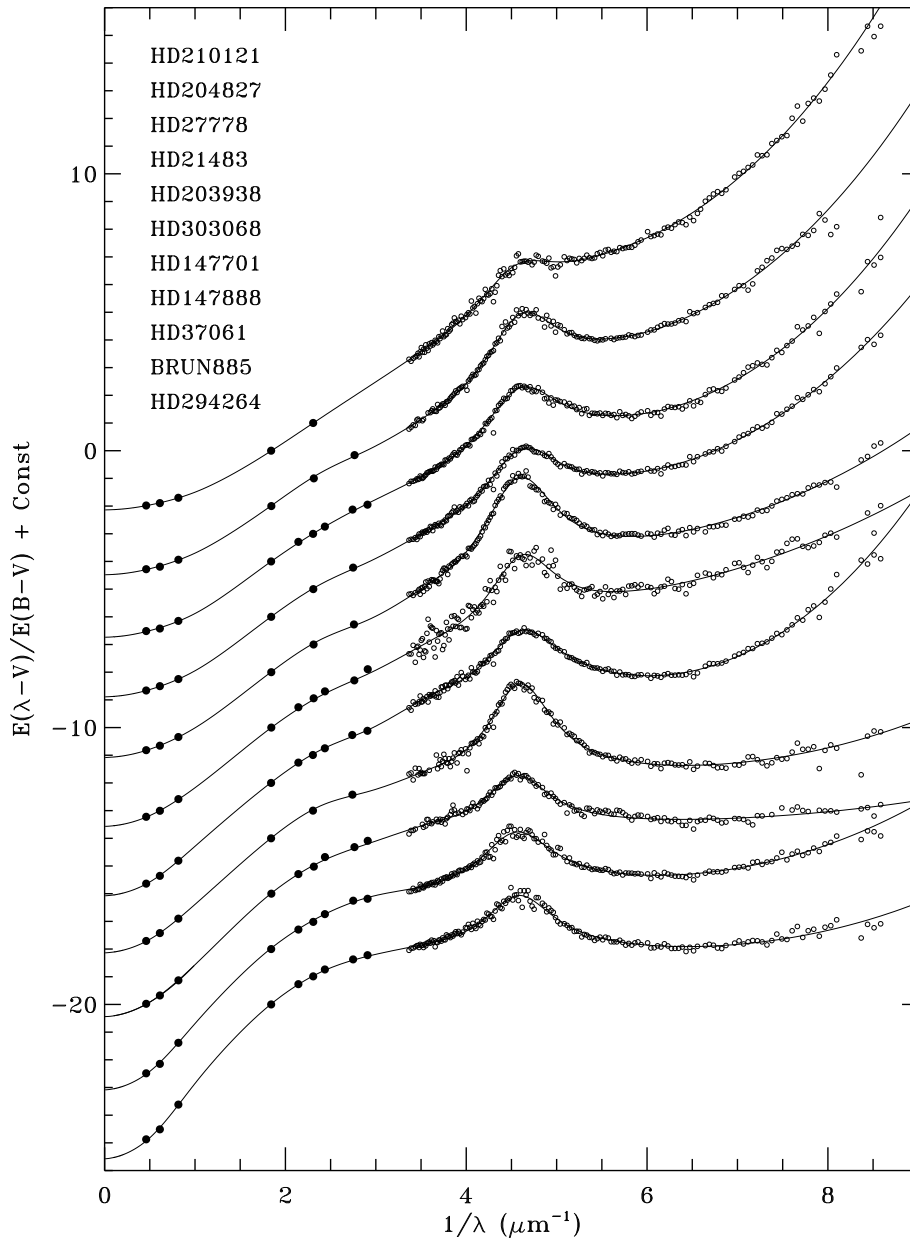


Fig. 5.— Examples of extinction curves produced with the SED fitting procedure. The smooth curves are the analytical representations of the extinction, which are determined by the fits. The data points show the actual ratios between the reddened star SEDs and the model atmosphere calculations. The curves have been successively offset downwards by 2 units for clarity. The data point at V ($1/\lambda = 1.83 \mu\text{m}^{-1}$) should be located at $E(\lambda - V)/E(B - V) = 0$ for each curve.

4.2. The Extinction Results

The primary results for the 96-star core sample are illustrated in Figures 6 through 11. While a full analysis of these data is yet to be performed, the major highlights can be summarized briefly:

- The IR extinction (i.e., at $\lambda > \sim 1 \mu\text{m}$) is well-represented by a power law of the form

$$A_\lambda/E(B - V) = k \times \lambda^{-\alpha}$$

with a universal exponent $\alpha = 1.84$ as suggested by Whittet (1992). The IR scale factor k varies smoothly and linearly with R_V , which ranges from ~ 2.1 to ~ 5.6 in the current sample. See Figure 6.

- In the UV, the position and FWHM of the 2175 Å bump are uncorrelated, consistent with the results of Fitzpatrick & Massa (1986). See Figure 7. The median value of the bump position for the core sample $4.59015 \mu\text{m}^{-1}$ (2178.6 Å) with a sample standard deviation of $0.020 \mu\text{m}^{-1}$. The median value of the FWHM is $0.92 \mu\text{m}^{-1}$ with a sample standard deviation of $0.11 \mu\text{m}^{-1}$.

- In the UV, the FWHM of the 2175 Å bump appears related to the strength of the nonlinear far-UV curvature, in the sense that broad bumps tend to be associated with large curvature. See Figure 8. This relationship is consistent with that presented by Fitzpatrick & Massa (1988).

- In the UV, the slope and intercept of the linear extinction underlying the bump are well-correlated, consistent with the results of Fitzpatrick & Massa (1988). See Figure 9.

- The slope of the UV linear component and the value of R_V are related: curves with large R_V tend to have flat UV slopes and curves with small R_V tend to have steep slopes. See the lefthand panel in Figure 10. This is the basis of the relationship found by Cardelli et al. (1989) between UV and optical/IR extinction. Note that plots of R_V directly against the level of extinction in the UV, e.g., R_V^{-1} versus $E(1250-V)/E(B-V)$, look essentially identical to the lefthand panel in Figure 10, exhibiting the same degree of scatter.

- There is a weak relationship between the strength of the far-UV curvature and the value of R_V : for $R_V < \sim 3.3$ the curvature tends to increase with decreasing R_V , for $R_V > \sim 3.3$ there is no apparent trend. See the right panel in Figure 10.

- The strength of the 2175 Å bump, as measured in curves normalized by $E(B-V)$, varies over a wide range, but displays a distinct trend: the strongest bumps are found for curves with intermediate levels of far-UV extinction and the bump weakens progressively as the far-UV extinction strays in either direction from the intermediate values. See Figure 11. Since the level of far-UV extinction is related to R_V , this means that, in general, weak bumps are found along high- R_V and low- R_V sightlines, while strong bumps occur along medium- R_V sightlines.

The reader has undoubtedly noticed that the relationships among the various quantities in Figures 6 through 11 are not particularly impressive! The only true correlations are those between

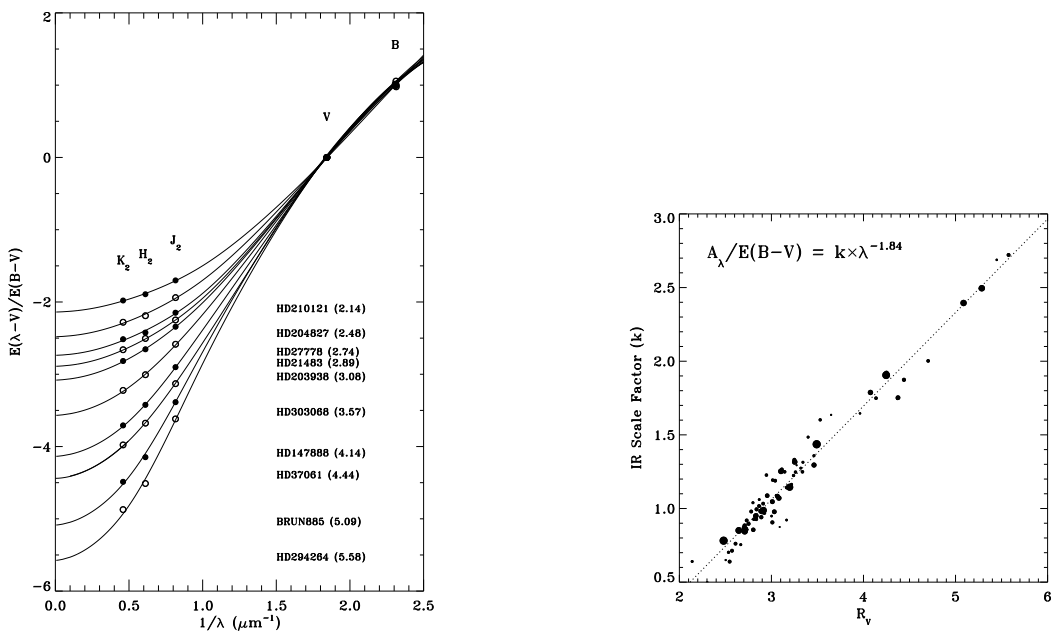


Fig. 6.— The lefthand panel shows the IR/optical extinction curves for 10 stars in the core sample. The stars and their R_V values are identified in the figure. The IR portion of the curves consist of power laws of the form $A_\lambda/E(B-V) = k \times \lambda^{-1.84}$ smoothly joined to the optical region with a cubic spline interpolation. The righthand panel shows that the IR scale factor k is a simple and well-correlated function of R_V . The dotted line is a linear least-squares fit corresponding to $k = 0.63R_V - 0.84$. The size of the symbols in the panel is proportional to the $E(B-V)$ of the sightline. Internal measurement errors are typically ± 0.03 for k and less than ± 0.1 for R_V .

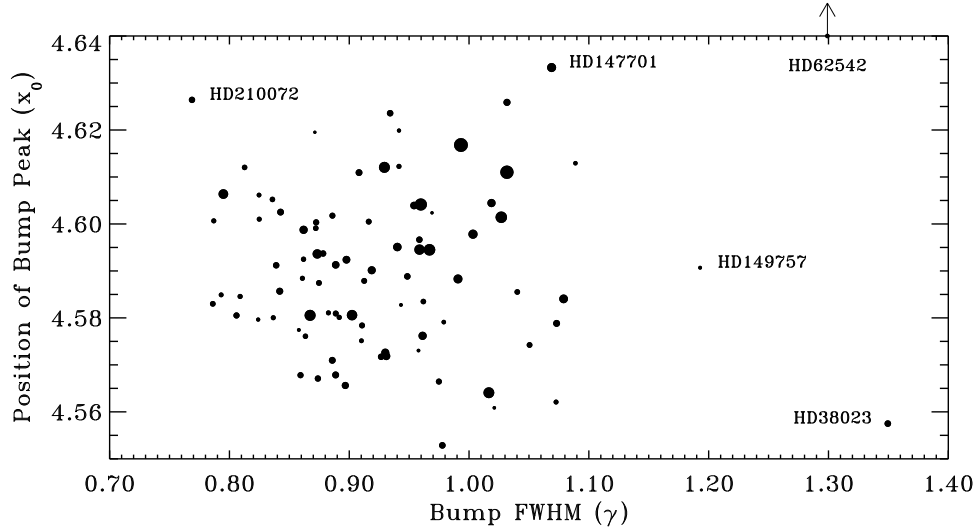


Fig. 7.— Plot of the FWHM γ of the 2175 Å bump versus the position of the bump peak x_0 , following the notation of Fitzpatrick & Massa 1990. Both quantities are in units of inverse microns, i.e., μm^{-1} . The size of the plot symbols in this and subsequent figures scales with $E(B-V)$. Typical internal measurement errors are $\pm 0.006 \mu\text{m}^{-1}$ for x_0 and $\pm 0.035 \mu\text{m}^{-1}$ for γ .

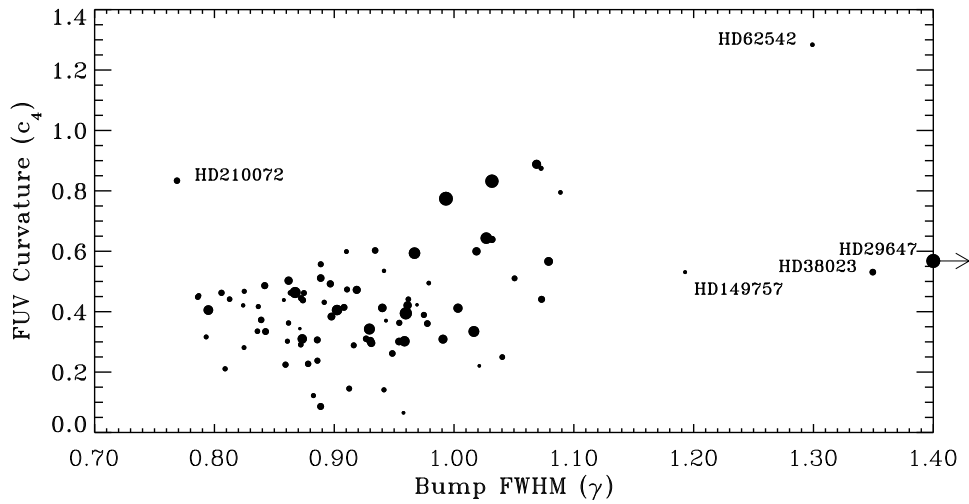


Fig. 8.— Plot of the FWHM γ of the 2175 Å bump versus the strength c_4 of the far-UV curvature. The typical internal measurement errors for c_4 are ± 0.04 .

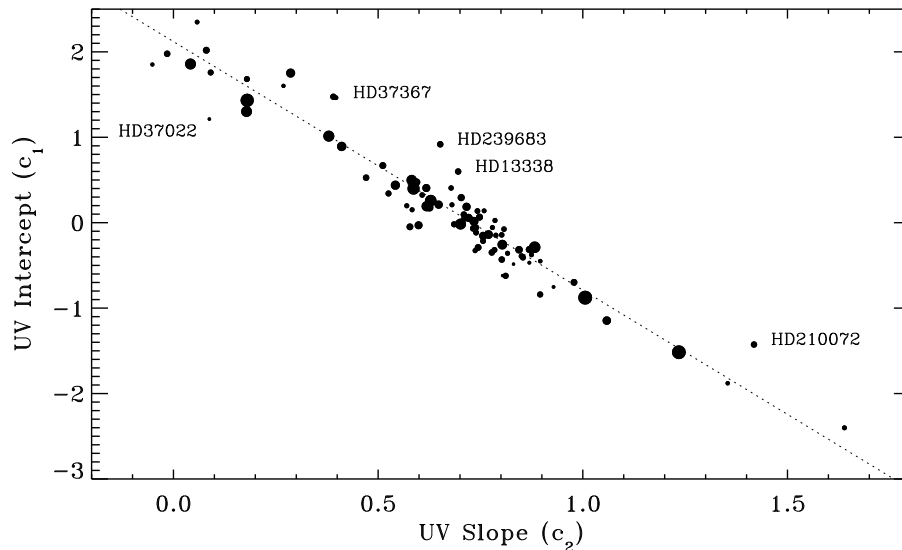


Fig. 9.— Plot of the slope of the UV linear extinction component c_2 versus its intercept c_1 . Typical internal measurements errors are ± 0.024 for c_2 and ± 0.11 for c_1 . The dotted line is a linear least-squares fit corresponding to $c_1 = 2.18 - 2.91c_2$.

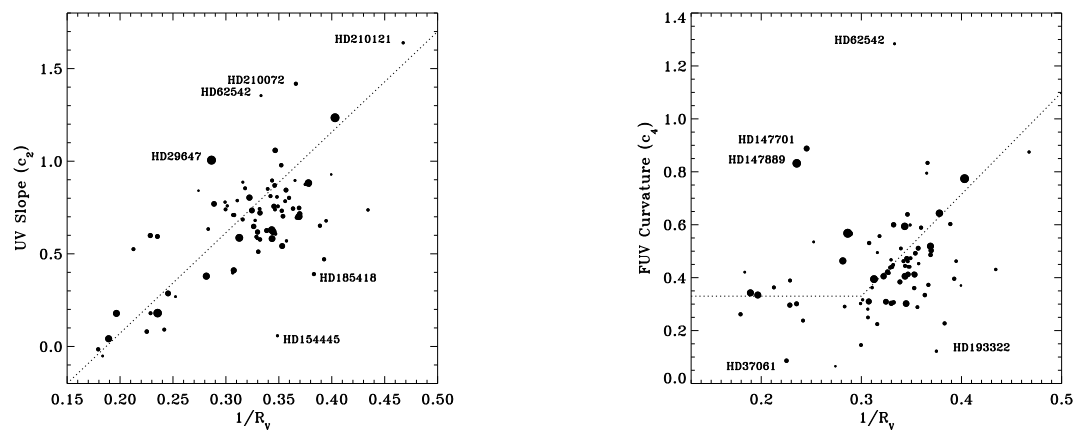


Fig. 10.— Plots of R_V^{-1} versus the slope c_2 of the UV linear extinction component (lefthand panel) and the strength c_4 of the far-UV curvature (right panel). The dotted lines in both panels are *not* formal fits to the data and are intended only to draw the eye to the general relationships between the quantities.

k and R_V in the optical/IR domain and between c_1 and c_2 in the UV domain. The trends seen among the other quantities are ill-defined — although, I believe, undoubtedly real — and characterized by an intrinsic scatter much larger than observational errors.

My primary conclusion derived from these data is that IR-through-UV Galactic extinction curves *should not be considered as a simple 1-parameter family*, whether characterized by R_V or any other quantity. While it is straightforward to create a family of curves which follow the trends established in Figures 6 through 11 — and this family is shown in Figures 12 and 13 — there are actually very few “real” extinction curves which agree in detail with these idealized forms. This follows, but extends, the conclusion of Cardelli et al. (1989) that real deviations from the “mean law” exist — most curves actually deviate from the mean! Twenty years ago Massa et al. (1983) made the comment that “peculiar extinction is common,” referring to the wide range of observed curve types. I think this statement should be amended to read “normal extinction is common,” with the understanding that “normal” actually covers a lot of territory! The truly peculiar curves, i.e., those which really stand out from the crowd in Figures 6 through 11, are actually rather rare.

4.3. The Interpretation

The data presented above raise a number of interesting issues which, as an observer, I feel no obligation to either interpret or understand. However there are a small number of rather obvious points and suggestions which might help illuminate some of the trends seen.

- *Size Distribution Matters...* The basic structure and the multiwavelength coherence seen in the IR-through-UV curves are determined primarily by 1) the IR power law (Figure 6), 2) the UV linear slope vs. linear intercept correlation (Figure 9), and 3) the relation between R_V and the UV slope (Figure 10). These three combine such that — as can be seen clearly in Figure 13 — large- R_V curves roll over in the optical and flatten out in the near-UV while small- R_V curves remain steep throughout the optical and into the UV. Since basic theoretical expectations (e.g., see Spitzer 1978, Fig. 7.1) show that extinction becomes grey in the regime where grains are large compared to the photon wavelengths, the observations imply that the connection between UV and IR extinction first noted by Cardelli et al. (1988, 1989) is simply a product of the grain size distribution. The large- R_V curves reflect sightlines with larger-than-typical mean grain sizes, while the small- R_V sightlines reflect smaller-than-typical mean grain sizes. If the relationship between R_V and UV extinction were a tight correlation, then we might be in the uncomfortable position of having to explain a remarkable uniformity in the form of the grain size distribution among widely varying sightlines. However, the observed scatter in Figure 10 probably indicates that Nature actually varies both the high- and low-end size cutoffs and the shape of the grain size distribution, producing a range in UV slopes for the same value of R_V , and a range of R_V 's for the same UV slope.

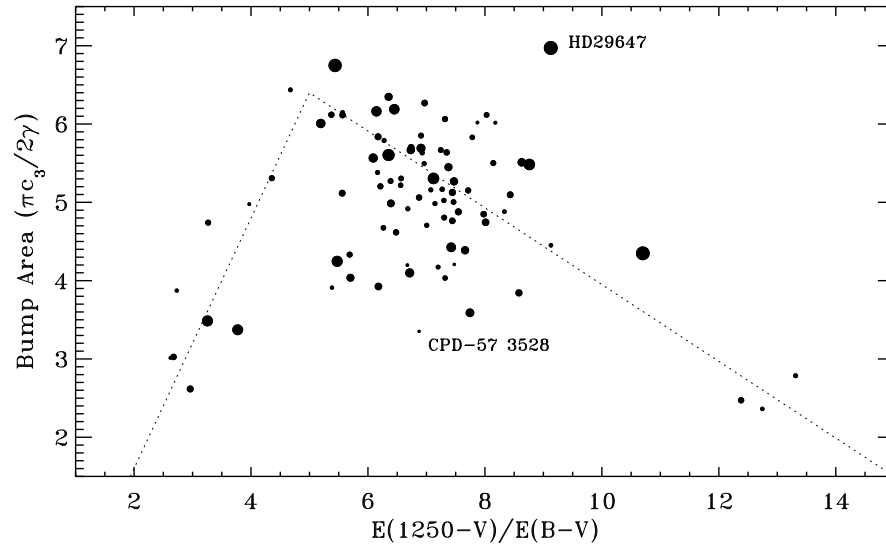


Fig. 11.— Plot of far-UV extinction level $E(1250-V)/E(B-V)$ versus the area of the 2175 Å bump in $E(\lambda-V)/E(B-V)$ extinction curves. The dotted line is intended only to illustrate the general relationship between the quantities.

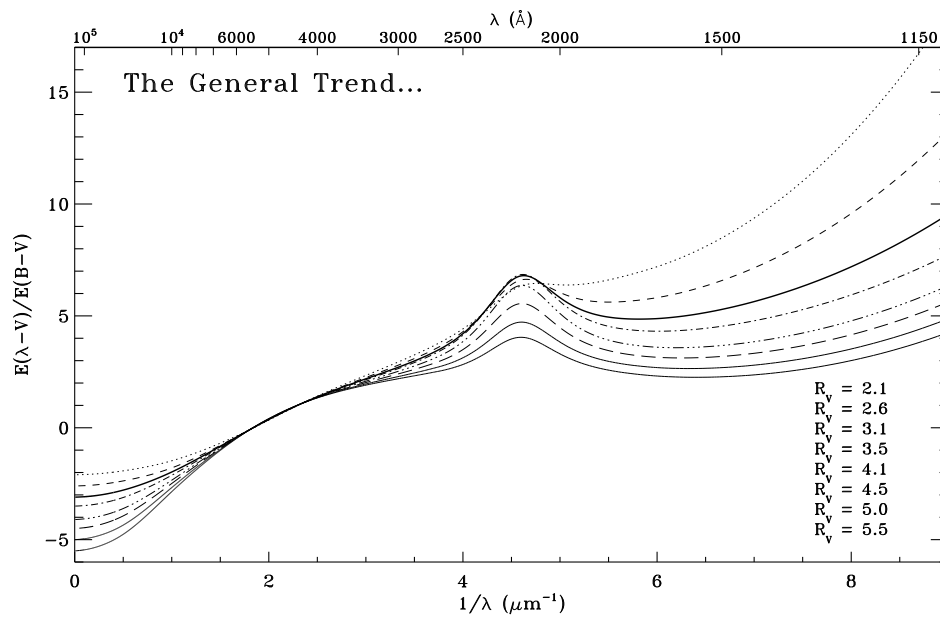


Fig. 12.— A set of normalized extinction curves, ranging from $R_V = 2.1$ to 5.5, which follow the general trends indicated by the dotted lines in Figures 6 through 11.

- *The Weak Bumps I...* The trend of weakening 2175 Å bump with increasing normalized far-UV extinction (and, thus, decreasing R_V) seen in Figure 11 might also be attributable to the grain size distribution. Because of the intrinsic steepness of their extinction in the optical region, grain populations which produce the high far-UV (low R_V) curves are very efficient producers of the optical color excess $E(B-V)$. In addition, such populations have a larger mean ratio of grain surface area (which is important for producing extinction) to grain mass, due to their smaller-than-average size distribution. As a result of these two effects, the grain populations which produce low R_V extinction probably have a much larger ratio of $E(B-V)$ per unit grain mass than high R_V populations. Since we normalize the curves by $E(B-V)$ it is possible that the grain populations which produce the steep, “weak-bumped” curves could actually have the same average bump strength per unit grain mass as in other sightlines. I.e., the apparent weakness of the bump could be an artifact of the normalization. Testing this will require measuring the bump strength relative to some absolute measure of the amount of grain material present along a line of sight, rather than to $E(B-V)$.

- *The Weak Bumps II...* The weakening of the bump in the flattest (highest R_V) extinction curves requires a different explanation than suggested above for the steepest curves. The highest R_V curves in the current sample are all associated with sightlines close to the Orion Trapezium region or towards the young O star Herschel 36. The extinction-producing material is likely freshly exposed to the interstellar radiation field, having only recently been deeply embedded in star-forming molecular clouds. By virtue of their opacity, we know essentially nothing about the UV extinction properties in such regions. It is not possible to say if the weak bumps observed in the large- R_V sightlines are typical of the opaque molecular regions, or are a result of some specific physical processes operating in their environments.

- *Beyond the Milky Way...* Having had a long-standing interest in the problem, I cannot resist violating the main constraint on this article and commenting on extinction outside the Milky Way galaxy — in the Magellanic Clouds, to be specific. The steep, weak-bumped extinction curves of the Large Cloud (LMC) and the really steep, really weak-bumped curves of the Small Cloud (SMC) have been a puzzle for 20 years. Observationally, the situation hasn’t changed much (qualitatively, at least) since I talked about these galaxies at the Santa Clara dust meeting in 1988. Theoretically, the idea that these curves are somehow the result of the progressively lower metal abundances of the LMC and SMC has been on the table — but unverified — since the first observations.

Figure 14 shows a comparison between extinction curves from the Galactic “family” featured in Figures 12 and 13 and the Magellanic Clouds. The very steep SMC curve has no known Galactic counterparts but — as seen in the figure — it represents only a slight extrapolation (to $R \simeq 1.9$) of the trends shown in Figures 10 and 11. The only notable discrepancies in the comparison are in the strength of the LMC bumps, which are each $\sim 30\%$ weaker than in the corresponding Galactic curves.

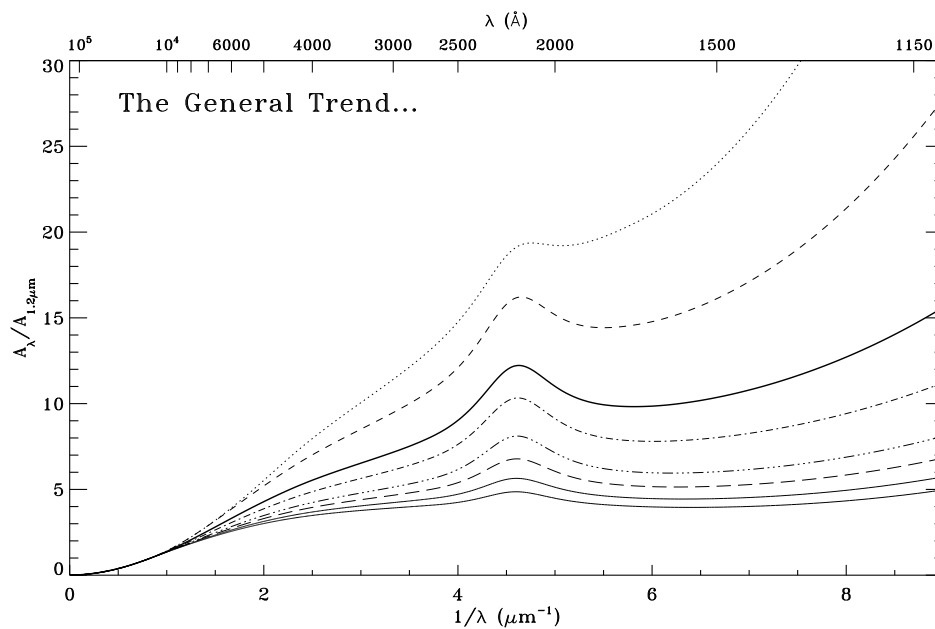


Fig. 13.— The same set of extinction curves as shown in Figure 12, but presented as total extinction A_λ normalized by $A_{1.2\mu m}$, the total extinction at $1.2 \mu m$.

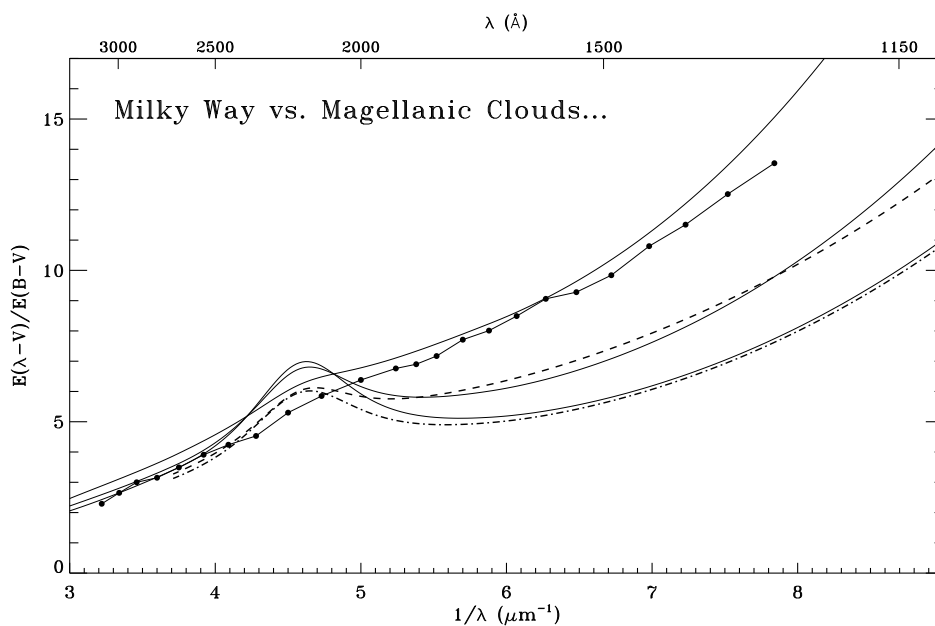


Fig. 14.— A comparison between idealized Galactic extinction curves with $R = 1.9$, 2.5 , and 2.85 and the SMC curve from Prévot et al. (1984; filled circles), the 30 Doradus curve (dashed curve), and the mean LMC curve (dash-dotted curve), respectively. The latter two curves are from Fitzpatrick (1986), as parametrized by Fitzpatrick & Massa (1990).

The results in Figure 14 are very suggestive and lead to an alternate explanation for Magellanic Cloud extinction: *the general properties of the LMC and SMC curves merely reflect the grain size distributions along their sightlines and aren't necessarily special products of alien extra-Galactic environments.* This is an appealingly simple idea, and also provides a straightforward explanation for the presence of sightlines in both galaxies which exhibit Galactic-like extinction: these are merely sightlines along which the mean grain size is similar to that along typical Galactic sightlines. There may well be some galaxy-specific details in the curves, perhaps the slightly weak LMC bumps, but, overall, these curves do not stand out in a qualitative sense from the Galactic sample.

If this suggestion is correct then the R_V values found in these galaxies should be low as compared with the Galactic mean. This is not obviously the current observational situation (e.g., see the recent results of Gordon et al. 2003) but I believe that R_V is so difficult to measure reliably for the lightly-reddened supergiants observed in the Clouds that the current observations do not at all rule out the grain-size explanation for Magellanic Cloud extinction. Note that Rodrigues et al. (1997) have already reached the conclusion, based on polarization and other data, that SMC grains are smaller than Galactic grains — except along the SMC sightline which exhibits Galactic-like UV extinction. In addition, a number of authors have modeled Magellanic Cloud extinction and shown that modified grain size distributions provide a plausible explanation for the observed curves (e.g., Pei 1992; Weingartner & Draine 2001; Clayton et al. 2003a). The contribution here is simply to point out that Magellanic Cloud extinction is consistent in general with trends observed along Galactic sightlines where the mean grain size is probably smaller-than-average.

- *Maybe It's Better Than It Looks...* Finally, it is possible that a number of effects conspire to make the various extinction properties appear less correlated with each other than they really are. I have screened the sample for obvious stellar peculiarities, which might distort the shape of the derived curves, but more difficult-to-diagnose problems may still exist for some curves. In addition, significant circumstellar material might be present in the vicinity of some of the stars, resulting in light scattered into the line of sight. Both these issues can be addressed by more detailed examination of the stellar data. Lastly, there is little doubt that some of the observed scatter arises because some sightlines traverse multiple regions of greatly different dust grain properties, e.g., a $R_V = 2.5$ region and a $R_V = 4.5$ region. Such superpositions will distort correlations between extinction properties which are related in an intrinsically non-linear way, as in Figures 10 and 11, but will not distort intrinsically linear correlations, as in Figures 6 and 9. For example, even if the strength of the 2175 Å bump were perfectly correlated with the far-UV extinction in the manner suggested by the dotted diagonal lines in Figure 11, the region between the diagonals would still be filled-in as a result of composite sightlines. With our larger sample of curves, Massa and I will attempt to identify composite sightlines and see if the some of the extinction properties are intrinsically better-related that first glance suggests.

5. Other Extinction Issues

By using virtually all my allotted space (and available energy!) concentrating on the issue of the “1-parameter family” I have slighted much recent work and many other researchers working hard on Galactic extinction-related issues. I cannot correct this fault in the small amount of remaining space, but do want to conclude by noting some currently active areas of investigation:

- *Far-UV Extinction...* Measurements of extinction in the 1150–912 Å region are very difficult due the presence of the Lyman-series absorption lines of H I and the Lyman- and Werner-series absorption bands of H_2 . In addition, heavy line-blanketing in the spectra of the early-type stars required for extinction measurements make the results very sensitive to spectral mismatch error. Recent results have been published by Hutchings & Giasson (2001), based on *FUSE* data, and Sasseen et al. (2002) based on *ORPHEUS* data. At this point, the far-UV extinction appears to be a smooth extrapolation of the rise seen in the mid-UV range, with no sign of a turnover. Much work remains to be done in this wavelength range.

- *Extinction Features...* The 2175 Å bump is the strongest observed extinction feature. Other dust-related spectroscopic features include the optical Diffuse Interstellar Bands and the IR solid-state emission and absorption bands. Clayton et al. (2003b) recently performed a detailed search in the UV for other extinction-related features, particularly as might be associated with absorption by polycyclic aromatic hydrocarbons. They found no evidence for such features down to a 3σ detection limit of $0.02A_V$. If these results (based on two lines of sight) are the norm, then UV extinction curves are evidently very, very smooth.

The optical and near-IR spectral regions would benefit from a similar study. For years there have been tantalizing hints of structure in the V band region, known as the “Very Broad Structure” or “VBS” (van Breda & Whittet 1982; Bastiaansen 1992) but no definitive characterization of its properties. This lack of data on an apparently observationally-accessible portion of the spectrum is undoubtedly due the inherent difficulties in obtaining precise ground-based spectrophotometry.

- *Morphology...* Despite many years of study, our understanding of extinction and its relationship with dust grain properties and environments still relies heavily on simple morphological investigations, e.g., Figures 6–11 of this paper. Such studies also include expanding the range of interstellar environments in which extinction is measured, as well as searching for relationships between extinction and other measurable quantities in the ISM. Recent work along these lines includes the Clayton, Gordon, & Wolff (2000) study of low density sightlines in the Milky Way and comparisons between the extinction properties along specific sightlines and their molecular content (Burgh et al 2000; Rachford et al. 2002).

By the time the next interstellar dust meeting rolls around, it is likely that studies such as these few examples listed above will have greatly improved our ability to characterize extinction as a function of interstellar environment and provided valuable insight into the natures of interstellar

grains and the processes which modify them.

REFERENCES

- Bastiaansen, P.A. 1992, *A&AS*, 93, 449
- Burgh, E.B., McCandless, S.R., Andersson, B-G, & Feldman, P.D. 2000, *ApJ*, 541, 250
- Cardelli, J.A., Clayton, G.C., & Mathis, J.S. 1988, *ApJ*, 329, L33
- Cardelli, J.A., Clayton, G.C., & Mathis, J.S. 1989, *ApJ*, 345, 245
- Clayton, G.C., & Fitzpatrick, E.L. 1987, *AJ*, 92, 157
- Clayton, G.C., Gordon, K.D., & Wolff, M.J. 2000, *ApJS*, 129, 147
- Clayton, G.C., et al. 2003a, *ApJ*, 588, 571
- Clayton, G.C., et al. 2003b, *ApJ*, 592, 947
- Draine, B.T. 1995, in *ASP Conf. Ser. Vol. 80, The Physics of the Interstellar Medium and Inter-galactic Medium*, eds. A. Ferrara, C.F. McKee, C. Heiles, & P.R. Shapiro (San Francisco: ASP), 133
- Draine, B.T. 2003, *ARA&A*, 41, (in press)
- Fitzpatrick, E.L. 1986, *AJ*, 92, 1068
- Fitzpatrick, E.L. 1999, *PASP*, 111, 63
- Fitzpatrick, E.L., & Massa, D.L. 1986, *ApJ*, 307, 286
- Fitzpatrick, E.L., & Massa, D.L. 1988, *ApJ*, 328, 734
- Fitzpatrick, E.L., & Massa, D.L. 1990, *ApJS*, 72, 163
- Fitzpatrick, E.L., & Massa, D.L. 1999, *ApJ*, 525, 1011
- Fitzpatrick, E. L., Ribas, I., Guinan, E. F., Maloney, F. P., & Claret, A. 2003 *ApJ*, 587, 685
- Gordon, K.D., Clayton, G.C., Misselt, K.A., Landolt, A.U., & Wolff, M.J. 2003, *ApJ*, in press
- Hutchings, J.B., & Giasson, J. 2001, *PASP*, 113, 1205
- Jenniskens, P., & Greenberg, J.M. 1993, *A&A*, 274, 439
- Johnson, H.L. 1965, *ApJ*, 141, 923
- Lanz, T., & Hubeny, I. 2003, *ApJS*, 146 (in press)

- Massa, D.L., & Savage, B.D. 1989, in IAU Symp. 135, Interstellar Dust, eds. L.J. Allamandola and A.G.G.M. Tielens (Dordrecht: Kluwer), 3
- Massa, D.L., Savage, B.D., & Fitzpatrick, E.L. 1983, *ApJ*, 266, 662
- Mathis, J.S., & Cardelli, J.A. 1992, *ApJ*, 398, 610
- Pei, Y.C. 1992, *ApJ*, 395, 130
- Prévot, M.L., Lequeux, J., Maurice, E., Prévot, L., & Rocca-Volmerange, B. 1984, *A&A*, 132, 389
- Rachford, B.L., et al. 2002, *ApJ*, 577, 221
- Rodrigues, C.V., Magalhães, A.M., Coyne, G.V., & Pirola, V. 1997, *ApJ*, 485, 618
- Sasseen, T.P., Hurwitz, M., Dixon, W.V., & Airieau, S. 2002, *ApJ*, 566, 267
- Savage, B.D. 1975, *ApJ*, 199, 92
- Savage, B.D., & Mathis, J.S. 1979, *ARA&A*, 17, 73
- Spitzer, L. 1978, *Physical Processes in the Interstellar Medium* (New York: Wiley-Interscience), 152
- Stecher, T.P. 1969, *ApJ*, 157, L125
- van Breda, I.G., & Whittet, D.C.B. 1981, *MNRAS*, 195, 79
- Weingartner, J.C., & Draine, B.T. 2001, *ApJ*, 548, 296
- Whittet, D.C.B. 1992, *Dust in the Galactic Environment* (Bristol: IOP Publishing)
- Whittet, D.C.B. 2003, *Dust in the Galactic Environment* 2nd ed. (Bristol: IOP Publishing)
- Witt, A. N., & Lillie, C.F. 1973, *A&A*, 25, 397